



CERN-EP-20XX-ZZZ
LHCb-PAPER-2021-052
December 10, 2021
v2r0

Observation of the doubly charmed baryon decay $\Xi_{cc}^{++} \rightarrow \Xi_c'^+ \pi^+$

LHCb collaboration[†]

Abstract

The $\Xi_{cc}^{++} \rightarrow \Xi_c'^+ \pi^+$ decay is observed using proton-proton collision data collected by the LHCb experiment at a centre-of-mass energy of 13 TeV, corresponding to an integrated luminosity of 5.6 fb^{-1} . The $\Xi_{cc}^{++} \rightarrow \Xi_c'^+ \pi^+$ decay is reconstructed partially, with the photon from the $\Xi_c'^+ \rightarrow \Xi_c^+ \gamma$ decay unreconstructed. The $\Xi_{cc}^{++} \rightarrow \Xi_c'^+ \pi^+$ branching fraction relative to that of the $\Xi_{cc}^{++} \rightarrow \Xi_c^+ \pi^+$ decay is measured to be $1.41 \pm 0.17 \pm 0.10$, where the first uncertainty is statistical and the second systematic.

To be submitted to JHEP

© 2021 CERN for the benefit of the LHCb collaboration. CC BY 4.0 licence.

[†]Authors are listed at the end of this paper.

1 Introduction

The quark model [1–3] predicts the existence of doubly charmed baryons that contain two charm quarks and a light quark (u, d, s), providing ideal systems to test models of quantum chromodynamics (QCD). In 2017, the LHCb collaboration reported the observation of the doubly charmed baryon Ξ_{cc}^{++} using the decay into the $\Lambda_c^+ K^- \pi^+ \pi^+$ final state, and measured its mass [4].¹ Such observation has been confirmed using the $\Xi_{cc}^{++} \rightarrow \Xi_c^+ \pi^+$ decay mode [5], following the proposal from Ref. [6]. The LHCb collaboration also measured the Ξ_{cc}^{++} lifetime [7] and the production rate [8], and searched for the $\Xi_{cc}^{++} \rightarrow D^+ p K^- \pi^+$ decay mode [9]. The Ξ_{cc}^{++} mass measurement has been updated [10] using both the $\Xi_{cc}^{++} \rightarrow \Lambda_c^+ K^- \pi^+ \pi^+$ and $\Xi_{cc}^{++} \rightarrow \Xi_c^+ \pi^+$ decays, based on a larger data sample recorded with improved trigger conditions.

This paper presents the observation of the $\Xi_{cc}^{++} \rightarrow \Xi_c'^+ \pi^+$ decay and the measurement of its branching fraction relative to that of the $\Xi_{cc}^{++} \rightarrow \Xi_c^+ \pi^+$ transition, using proton-proton (pp) collision data collected by the LHCb experiment at a centre-of-mass energy of 13 TeV, corresponding to an integrated luminosity of 5.6 fb^{-1} . The signal $\Xi_{cc}^{++} \rightarrow \Xi_c'^+ \pi^+$ decay is reconstructed partially, with the photon from the $\Xi_c'^+ \rightarrow \Xi_c^+ \gamma$ process unreconstructed. The Ξ_c^+ baryon is reconstructed with the $\Xi_c^+ \rightarrow p K^- \pi^+$ decay for both the signal and control modes.

This measurement can be used to test various theoretical models, by comparing the measured relative branching fraction to theoretical predictions, which take into account several aspects. Firstly, the internal structure and the weak decay model of the Ξ_{cc}^{++} state. It is difficult to take the three constituent quarks into account from a solid QCD analysis. An alternative way to simplify the problem is to treat two of them as a diquark system. There are two models based on this simplification. The first model assumes a $(cu)+c$ configuration, then the bachelor c -quark decays and the diquark remains as a spectator, leading to a prediction of the relative branching fraction of 0.7 [11]. The second model takes the $(cc)+u$ configuration with the diquark system breaking half way, leading to a $(cc)u \rightarrow c(su)$ transition and a predicted relative branching fraction of 0.56 ± 0.18 [12] or 0.30 ± 0.24 [13]. Secondly, the contribution of inner W -emission. Two topological diagrams will contribute to the $\Xi_{cc}^{++} \rightarrow \Xi_c'^+ \pi^+$ decay amplitude, as shown in Fig. 1, the external and internal W -emissions. Considering the inner W -emission diagram contribution, the relative branching fraction is predicted between 0.81 and 0.83 [14, 15]. Thirdly, the flavour wave function symmetry. The flavour wave function of the Ξ_{cc}^{++} and Ξ_c^+ baryons is antisymmetric, while for the $\Xi_c'^+$ state is symmetric, which implies that the $\Xi_{cc}^{++} \rightarrow \Xi_c^+$ transition is flavour symmetric while $\Xi_{cc}^{++} \rightarrow \Xi_c'^+$ is flavour antisymmetric. Predicted by the Körner-Pati-Woo (KPW) theorem [16, 17], the internal W -emission amplitude of the $\Xi_{cc}^{++} \rightarrow \Xi_c'^+$ transition is largely suppressed due to its flavour antisymmetry. Including the KPW theorem, the relative branching fraction is predicted to be 4.33 [18–20] or 4.55 [21]. Finally, the interference between factorizable and nonfactorizable contributions. When the interference between these two contributions for both S - and P -wave amplitudes are considered, the relative branching fraction is predicted to be 6.74 [22].

¹The inclusion of charge-conjugate particle/processes is implied throughout.

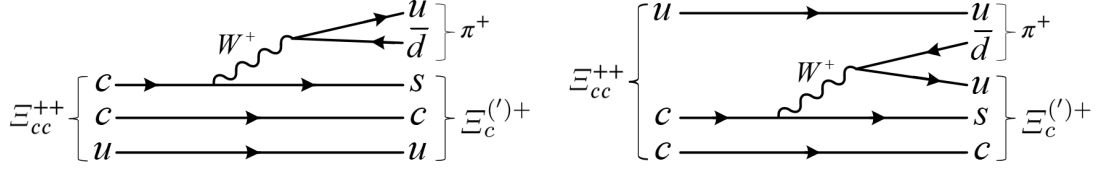


Figure 1: (Left) External and (right) internal W -emission Feynman diagrams of the $\Xi_{cc}^{++} \rightarrow \Xi_c^{(')+} \pi^+$ decay.

2 Detector and simulation

The LHCb detector [23, 24] is a single-arm forward spectrometer covering the pseudorapidity range $2 < \eta < 5$, designed for the study of particles containing b or c quarks. The detector includes a high-precision tracking system consisting of a silicon-strip vertex detector surrounding the pp interaction region, a large-area silicon-strip detector located upstream of a dipole magnet with a bending power of about 4 Tm, and three stations of silicon-strip detectors and straw drift tubes placed downstream of the magnet. The tracking system provides a measurement of the momentum, p , of charged particles with a relative uncertainty that varies from 0.5% at low momentum to 1.0% at 200 GeV/ c . The minimum distance of a track to a primary pp collision vertex, the impact parameter, is measured with a resolution of $(15 + 29/p_T) \mu\text{m}$, where p_T is the component of the momentum transverse to the beam, in GeV/ c . Different types of charged hadrons are distinguished using information from two ring-imaging Cherenkov detectors. Photons, electrons and hadrons are identified by a calorimeter system consisting of scintillating-pad and preshower detectors, an electromagnetic and a hadronic calorimeter. Muons are identified by a system composed of alternating layers of iron and multiwire proportional chambers.

The online event selection is performed by a trigger [25], which consists of a hardware stage, based on information from the calorimeter and muon systems, followed by a software stage, which applies a full event reconstruction. In between the two software stages, an alignment and calibration of the detector is performed in near real-time. This process allows the reconstruction of Ξ_{cc}^{++} decays to be performed entirely in the software trigger, whose output is used as input to the present analysis.

During the selection, trigger signals are associated with reconstructed particles. Selection requirements can therefore be made on the trigger selection itself and on whether the decision was due to the signal candidate (trigger on signal, TOS), or other particles produced in the pp collision (trigger independent on signal, TIS).

The simulation samples are used to model the effects of the detector acceptance and to estimate the efficiencies of the selection requirements. In the simulation, pp collisions are generated using PYTHIA [26] with a specific LHCb configuration [27]. A dedicated generator GENXICC2.0 [28] is used for the Ξ_{cc}^{++} production. Decays of unstable particles are described by EVTGEN [29], in which final-state radiation is generated using PHOTOS [30]. The interaction of the generated particles with the detector, and its response, are implemented using the GEANT4 toolkit [31]. Fast simulated samples with AMPGEN [32] and RAPIDSIM [33] toolkits are also used in this analysis. The simulated samples by AMPGEN are used to study the signal distribution with different amplitude hypotheses, while the RAPIDSIM samples are used to estimate various background decays

that may appear in the data, such as $\Xi_{cc}^{++} \rightarrow \Xi_c(2645/2790)^+ \pi^+$ decays.

3 Event selection

The reconstruction and event selection of the $\Xi_{cc}^{++} \rightarrow \Xi_c^{(')+} \pi^+$ decays are the same as in the previous LHCb analysis [10]. To give a brief summary, the particle identification (PID) are required on the final-state particles of the $\Xi_c^+ \rightarrow p K^- \pi^+$ decay and the pion from the $\Xi_{cc}^{++} \rightarrow \Xi_c^{(')+} \pi^+$ process. These tracks are required to form a common vertex of good-quality and be detached from the primary pp collision vertex. A Multilayer Perceptron (MLP) algorithm from the TMVA toolkit [34] is used to improve the signal purity.

Compared with the previous analysis [10], the data samples are further filtered into two disjoint subsamples using information from the hardware trigger. The first contains candidates that are triggered by at least one of the Ξ_c^+ decay products with high transverse energy deposited in the calorimeters (TOS). The second consists of events that are exclusively triggered by particles unrelated to the signal decay products; these events can, for example, be triggered by the decay products of the charmed hadrons produced together with the signal baryon (TIS).

4 Relative branching fraction measurement

To measure the branching fraction of the signal decay relative to that of the control channel, both the relative signal yields and efficiencies are needed, as defined below,

$$\frac{\mathcal{B}(\Xi_{cc}^{++} \rightarrow \Xi_c^{(')+} \pi^+)}{\mathcal{B}(\Xi_{cc}^{++} \rightarrow \Xi_c^+ \pi^+)} = \frac{N_{\Xi_c^{(')+}}}{N_{\Xi_c^+}} \times \frac{\epsilon_{\Xi_c^+}}{\epsilon_{\Xi_c^{(')+}}}, \quad (1)$$

where $N_{\Xi_c^{(')+}}$ stands for the signal yield of the $\Xi_{cc}^{++} \rightarrow \Xi_c^{(')+} \pi^+$ decay, and $\epsilon_{\Xi_c^{(')+}}$ represents the total efficiency for each decay. The relative signal yield is determined by fitting to the $\Xi_c^+ \pi^+$ invariant-mass spectrum in the data, and the relative efficiency is determined from fully simulated samples of signal and control decay modes. Before estimating the relative efficiency, kinematic distributions of the simulated samples are weighted to match those in the data.

A simultaneous, unbinned maximum likelihood fit is performed to the invariant mass distribution $M(\Xi_c^+ \pi^+) \equiv m(\Xi_c^+ \pi^+) - m(\Xi_c^+) + m_0(\Xi_c^+)$ in the TOS and TIS samples to determine the relative signal yield. Here, $m(\Xi_c^+ \pi^+)$ and $m(\Xi_c^+)$ are the reconstructed invariant masses of the Ξ_{cc}^{++} and Ξ_c^+ candidates, and $m_0(\Xi_c^+)$ is the known Ξ_c^+ mass [35].

Four components are considered in the fit model, for both TOS and TIS categories:

- $\Xi_{cc}^{++} \rightarrow \Xi_c^+ \pi^+$ decays, described by a Crystal Ball function [36], defined as

$$f(x|\alpha, n, \bar{x}, \sigma) = \begin{cases} e^{-\frac{(x-\bar{x})^2}{2\sigma^2}} & \text{for } \frac{x-\bar{x}}{\sigma} > -\alpha \\ \left(\frac{n}{|\alpha|}\right)^n e^{-\frac{|\alpha|^2}{2}} \left(\frac{n}{|\alpha|} - |\alpha| - \frac{x-\bar{x}}{\sigma}\right)^{-n} & \text{for } \frac{x-\bar{x}}{\sigma} \leq -\alpha, \end{cases} \quad (2)$$

where \bar{x} is the mean mass and σ the mass resolution. The parameters α and n describe the tail caused by the final-state radiation, and are parameterised as a function of the mass resolution as done in Ref. [10].

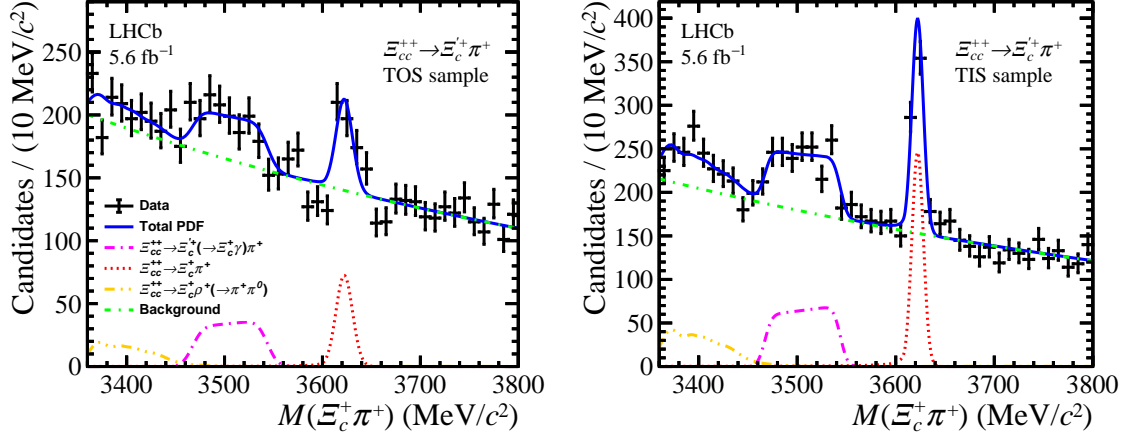


Figure 2: Invariant-mass distribution of the Ξ_{cc}^{++} candidates from the (left) TOS and (right) TIS samples, with fit results overlaid. The $\Xi_{cc}^{++} \rightarrow \Xi_c'^+ \pi^+$ component is shown as a purple dashed line, and the $\Xi_{cc}^{++} \rightarrow \Xi_c^+ \pi^+$ component as a red dotted line.

- $\Xi_{cc}^{++} \rightarrow \Xi_c'^+ \pi^+$ decays, parametrized by a box function describing the true mass distribution of the signal convoluted with a Gaussian resolution function. The upper and lower boundaries of the box are fixed by the kinematic ranges, while their slopes are fixed from the simulation. The resolution is the same as for the Crystal Ball function.
- Partially reconstructed background, due to $\Xi_{cc}^{++} \rightarrow \Xi_c^+ \rho^+ (\pi^+ \pi^0)$ decays. The $m(\Xi_c^+ \pi^+)$ distribution is taken from the fully simulated $\Xi_{cc}^{++} \rightarrow \Xi_c^+ \rho^+$ sample. The yields of the $\Xi_{cc}^{++} \rightarrow \Xi_c^+ \rho^+$ components in the TOS and TIS samples are related to each other by the relative efficiency.
- Combinatorial background, described by an exponential function. The slope of each exponential function is varied freely in the fit.

The invariant-mass distribution of the Ξ_{cc}^{++} candidates together with the fit results for the two trigger categories are shown in Fig. 2. The signal yields determined from the fit are listed in Table 1, giving the relative signal yields to be

$$\begin{aligned} \frac{N_{\Xi_c'^+}}{N_{\Xi_c^+}}|_{\text{TOS}} &= 1.6 \pm 0.4, \\ \frac{N_{\Xi_c'^+}}{N_{\Xi_c^+}}|_{\text{TIS}} &= 1.3 \pm 0.2, \end{aligned} \tag{3}$$

where the quoted uncertainties are statistical only.

To measure the relative efficiencies, fully simulated samples of the signal and control modes are used. The Ξ_{cc}^{++} lifetime in the simulation is weighted to the known Ξ_{cc}^{++} lifetime [35]. The Ξ_{cc}^{++} transverse momentum and the detector multiplicity are weighted to match those in the data. The data distributions are obtained for the TOS and TIS categories separately using the *sPlot* method [37], in the $M(\Xi_c^+ \pi^+)$ region between 3570 and 3680 MeV/c², where only the exclusive Ξ_{cc}^{++} signal peak and combinatorial background

are present. The fit model for these components is the same as described previously. The relative efficiencies are determined to be

$$\begin{aligned}\frac{\epsilon_{\Xi_c'^+}}{\epsilon_{\Xi_c^+}}|_{\text{TOS}} &= (90.5 \pm 4.1)\%, \\ \frac{\epsilon_{\Xi_c'^+}}{\epsilon_{\Xi_c^+}}|_{\text{TIS}} &= (97.2 \pm 3.5)\%,\end{aligned}\tag{4}$$

where the uncertainties are statistical only due to the limited size of the simulated samples.

5 Systematic uncertainties

The relative branching fraction measurement is affected by systematic uncertainties arising from determinations of the relative signal yields and efficiencies, as summarised in Table 2.

Uncertainties from the determination of the relative signal yields are caused by imperfect modeling of each component in the fit. To estimate such effects, alternative models are used replacing the corresponding components discussed in Sec. 4 and the changes of the relative signal yields are taken as systematic uncertainties. The alternative signal model uses the distribution from the fully simulated signal sample instead of the box function convoluted with the resolution function, leading to a systematic uncertainty of 4.9% (0.8%) for the TOS (TIS) sample. The alternative model for the control decay mode is a Crystal Ball function with the tail parameters α and n varied in the fit, leading to a systematic uncertainty of 3.7% (3.8%) for the TOS (TIS) sample. For the combinatorial background, a second-order polynomial function is used, and a systematic uncertainty of 0.6% (3.1%) is assigned.

To estimate the uncertainties from partially reconstructed background, the following decay channels are generated using the fast simulation toolkit and assuming different angular momentum hypotheses (S -, P -, D -wave or a mixture if possible):

- $\Xi_{cc}^{++} \rightarrow \Xi_c^+ \rho^+$, $\rho^+ \rightarrow \pi^+ \pi^0$ decays are generated phase space for the default fit. More angular momentum hypotheses are tested.
- $\Xi_{cc}^{++} \rightarrow \Xi_c^+ \pi^+ \pi^0$ without intermediate states, with the neutral pion missing in the reconstruction.
- $\Xi_{cc}^{++} \rightarrow \Xi_c(2645)^+ \pi^+$, $\Xi_c(2645)^+ \rightarrow \Xi_c^+ \pi^0$, with the neutral pion missing.
- $\Xi_{cc}^+ \rightarrow \Xi_c(2645)^0 \pi^+$, $\Xi_c(2645)^0 \rightarrow \Xi_c^+ \pi^-$, with the negatively charged pion missing.
- $\Xi_{cc}^{++} \rightarrow \Xi_c(2790)^+ \pi^+$, $\Xi_c(2790)^+ \rightarrow \Xi_c'^+ \pi^0$ decays, with both the photon and the neutral pion missing.

Table 1: Yields of the signal and normalisation modes.

Category	$\Xi_{cc}^{++} \rightarrow \Xi_c'^+ \pi^+$	$\Xi_{cc}^{++} \rightarrow \Xi_c^+ \pi^+$
TOS	262 ± 53	159 ± 32
TIS	494 ± 63	379 ± 32

Table 2: Relative systematic uncertainties on the branching fraction ratio $\frac{\mathcal{B}(\Xi_{cc}^{++} \rightarrow \Xi_c'^+ \pi^+)}{\mathcal{B}(\Xi_{cc}^{++} \rightarrow \Xi_c^+ \pi^+)}$.

Source	TOS [%]	TIS [%]
Signal model	4.9	0.8
Control model	3.7	3.8
Combinatorial background	0.6	3.1
Partially reconstructed background	3.7	1.5
Mass window	11.0	3.9
Simulated sample size	4.5	3.6
Kinematic corrections	0.5	1.8
Particle identification	0.5	0.7
Sum in quadrature	13.9	7.7

- $\Xi_{cc}^{++} \rightarrow \Xi_c(2815)^+ \pi^+$, $\Xi_c(2815)^+ \rightarrow \Xi_c(2645)^+ \pi^0$ decays, with two neutral pions missing.

The tests reveal that including the top two sources the fits give similar results as reported in Sec. 4, the statistical significance of the third and forth decay modes is less than two standard deviations, and the $M(\Xi_c^+ \pi^+)$ distributions of the last two decay modes are outside the mass window used in this analysis and can be ignored. Including all sources of the partially reconstructed background, the largest deviation from the default relative signal yields reported in Sec. 4 is taken as systematic uncertainty, amounting to 3.7% (1.5%) for the TOS (TIS) sample.

Uncertainties due to the range of the chosen mass window are also evaluated. The $M(\Xi_c^+ \pi^+)$ upper sideband contains only combinatorial background and is simple to describe, thus only the effects from the low mass window boundary are considered. The low mass window boundary is scanned from 3350 to 3450 MeV/ c^2 , and the largest deviation from the default relative signal yield is taken as a systematic uncertainty, leading to 11.0% (3.9%) for the TOS (TIS) sample. Although this is the largest contribution among all the systematic uncertainties, the relative branching fraction is still dominated by the statistical uncertainty.

Three sources of systematic uncertainty arising from the determination of the relative efficiencies are evaluated. First, the uncertainties due to limited size of the simulated samples, which contribute 4.5% (3.6%) for the TOS (TIS) sample. The second is due to the kinematic corrections to the simulation. The uncertainties due to both weighting method and limited size of the background-subtracted data are considered. The relative uncertainty is less than 1% for the TOS and 1.8% for the TIS samples. The last contribution arises from uncertainties on the PID efficiency and is studied using PID calibration samples [38]. The relative uncertainty is found to be less than 1% for both the TOS and TIS samples. As the signal and control decay modes have the same final states and very similar kinematic distributions, other systematic sources, such as the tracking and trigger efficiencies, cancel out in the ratio and are found to be negligible.

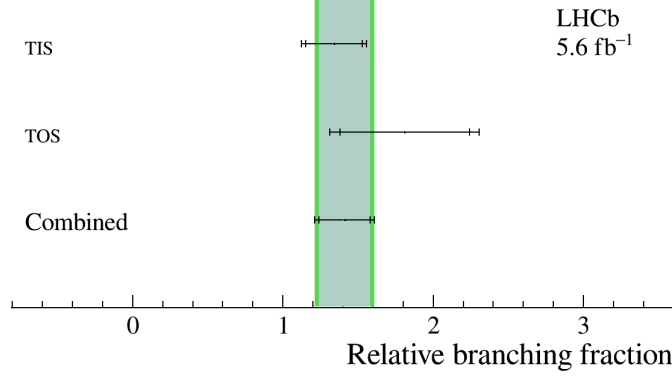


Figure 3: Measured relative branching fraction for the TOS and TIS samples and the combined result. The inner error bars represent statistical uncertainties and the outer error bars represent the total uncertainties.

6 Results and summary

Including all systematic uncertainties, the measured relative branching fraction in the TOS and TIS samples are

$$\begin{aligned} \frac{\mathcal{B}(\Xi_{cc}^{++} \rightarrow \Xi_c'^+ \pi^+)}{\mathcal{B}(\Xi_{cc}^{++} \rightarrow \Xi_c^+ \pi^+)}|_{\text{TOS}} &= 1.81 \pm 0.43 \pm 0.25, \\ \frac{\mathcal{B}(\Xi_{cc}^{++} \rightarrow \Xi_c'^+ \pi^+)}{\mathcal{B}(\Xi_{cc}^{++} \rightarrow \Xi_c^+ \pi^+)}|_{\text{TIS}} &= 1.34 \pm 0.19 \pm 0.10, \end{aligned} \quad (5)$$

where the first uncertainty is statistical and the second systematic. The combination of the two measurements is performed using the Best Linear Unbiased Estimator (BLUE) [39,40]. The combined result is

$$\frac{\mathcal{B}(\Xi_{cc}^{++} \rightarrow \Xi_c'^+ \pi^+)}{\mathcal{B}(\Xi_{cc}^{++} \rightarrow \Xi_c^+ \pi^+)} = 1.41 \pm 0.17 \pm 0.10. \quad (6)$$

In the combination, uncertainties arising from the modelling of the signal and control modes, combinatorial background and partially reconstructed background, are assumed to be 100% correlated between the TOS and TIS samples, while the rest are taken to be uncorrelated. The individual relative branching fractions of the TOS and TIS samples and the combined result are illustrated in Fig. 3.

In summary, a new decay mode of the doubly charmed baryon $\Xi_{cc}^{++} \rightarrow \Xi_c'^+ \pi^+$ is observed in a data sample of pp collisions collected by the LHCb experiment at centre-of-mass energy of $\sqrt{s} = 13$ TeV, corresponding to an integrated luminosity of 5.6 fb^{-1} . This is the third observed decay mode of the Ξ_{cc}^{++} baryon following the $\Xi_{cc}^{++} \rightarrow \Lambda_c^+ K^- \pi^+ \pi^+$ [4] and $\Xi_{cc}^{++} \rightarrow \Xi_c^+ \pi^+$ [5] decays. The relative branching fraction between the $\Xi_{cc}^{++} \rightarrow \Xi_c'^+ \pi^+$ and $\Xi_{cc}^{++} \rightarrow \Xi_c^+ \pi^+$ decays is measured for the first time. The result is not yet described by all the theoretical predictions [11–15, 18–22].

Acknowledgements

We express our gratitude to our colleagues in the CERN accelerator departments for the excellent performance of the LHC. We thank the technical and administrative staff at the

LHCb institutes. We acknowledge support from CERN and from the national agencies: CAPES, CNPq, FAPERJ and FINEP (Brazil); MOST and NSFC (China); CNRS/IN2P3 (France); BMBF, DFG and MPG (Germany); INFN (Italy); NWO (Netherlands); MNiSW and NCN (Poland); MEN/IFA (Romania); MSHE (Russia); MICINN (Spain); SNSF and SER (Switzerland); NASU (Ukraine); STFC (United Kingdom); DOE NP and NSF (USA). We acknowledge the computing resources that are provided by CERN, IN2P3 (France), KIT and DESY (Germany), INFN (Italy), SURF (Netherlands), PIC (Spain), GridPP (United Kingdom), RRCKI and Yandex LLC (Russia), CSCS (Switzerland), IFIN-HH (Romania), CBPF (Brazil), PL-GRID (Poland) and NERSC (USA). We are indebted to the communities behind the multiple open-source software packages on which we depend. Individual groups or members have received support from ARC and ARDC (Australia); AvH Foundation (Germany); EPLANET, Marie Skłodowska-Curie Actions and ERC (European Union); A*MIDEX, ANR, IPhU and Labex P2IO, and Région Auvergne-Rhône-Alpes (France); Key Research Program of Frontier Sciences of CAS, CAS PIFI, CAS CCEPP, Fundamental Research Funds for the Central Universities, and Sci. & Tech. Program of Guangzhou (China); RFBR, RSF and Yandex LLC (Russia); GVA, XuntaGal and GENCAT (Spain); the Leverhulme Trust, the Royal Society and UKRI (United Kingdom).

References

- [1] M. Gell-Mann, *A schematic model of baryons and mesons*, Phys. Lett. **8** (1964) 214.
- [2] G. Zweig, *An SU_3 model for strong interaction symmetry and its breaking; Version 1* CERN-TH-401, CERN, Geneva, 1964.
- [3] G. Zweig, *An SU_3 model for strong interaction symmetry and its breaking; Version 2* CERN-TH-412, CERN, Geneva, 1964.
- [4] LHCb collaboration, R. Aaij *et al.*, *Observation of the doubly charmed baryon Ξ_{cc}^{++}* , Phys. Rev. Lett. **119** (2017) 112001, [arXiv:1707.01621](#).
- [5] LHCb collaboration, R. Aaij *et al.*, *First observation of the doubly charmed baryon decay $\Xi_{cc}^{++} \rightarrow \Xi_c^+ \pi^+$* , Phys. Rev. Lett. **121** (2018) 162002, [arXiv:1807.01919](#).
- [6] F.-S. Yu *et al.*, *Discovery potentials of doubly charmed baryons*, Chin. Phys. **C42** (2018) 051001, [arXiv:1703.09086](#).
- [7] LHCb collaboration, R. Aaij *et al.*, *Measurement of the lifetime of the doubly charmed baryon Ξ_{cc}^{++}* , Phys. Rev. Lett. **121** (2018) 052002, [arXiv:1806.02744](#).
- [8] LHCb collaboration, R. Aaij *et al.*, *Measurement of Ξ_{cc}^{++} production in pp collisions at $\sqrt{s} = 13$ TeV*, Chin. Phys. **C44** (2020) 022001, [arXiv:1910.11316](#).
- [9] LHCb collaboration, R. Aaij *et al.*, *A search for $\Xi_{cc}^{++} \rightarrow D^+ p K^- \pi^+$ decays*, JHEP **10** (2019) 124, [arXiv:1905.02421](#).
- [10] LHCb collaboration, R. Aaij *et al.*, *Precision measurement of the Ξ_{cc}^{++} mass*, JHEP **02** (2020) 049, [arXiv:1911.08594](#).

- [11] W. Wang, F.-S. Yu, and Z.-X. Zhao, *Weak decays of doubly heavy baryons: the $1/2 \rightarrow 1/2$ case*, Eur. Phys. J. **C77** (2017) 781, [arXiv:1707.02834](#).
- [12] H.-W. Ke, F. Lu, X.-H. Liu, and X.-Q. Li, *Study on $\Xi_{cc} \rightarrow \Xi_c$ and $\Xi_{cc} \rightarrow \Xi'_c$ weak decays in the light-front quark model*, Eur. Phys. J. **C80** (2020) 140, [arXiv:1912.01435](#).
- [13] Y.-J. Shi, W. Wang, and Z.-X. Zhao, *QCD Sum Rules analysis of weak decays of doubly-heavy baryons*, Eur. Phys. J. **C80** (2020) 568, [arXiv:1902.01092](#).
- [14] N. Sharma and R. Dhir, *Estimates of W -exchange contributions to Ξ_{cc} decays*, Phys. Rev. **D96** (2017) 113006, [arXiv:1709.08217](#).
- [15] A. S. Gerasimov and A. V. Luchinsky, *Weak decays of doubly heavy baryons: Decays to a system of π mesons*, Phys. Rev. **D100** (2019) 073015, [arXiv:1905.11740](#).
- [16] J. G. Korner, *Octet behaviour of single-particle matrix elements $\langle B' | H_W | B \rangle$ and $\langle M' | H_W | M \rangle$ using a weak current-current quark Hamiltonian*, Nucl. Phys. **B25** (1971) 282.
- [17] J. C. Pati and C. H. Woo, *$\Delta I = \frac{1}{2}$ rule with fermion quarks*, Phys. Rev. **D3** (1971) 2920.
- [18] T. Gutsche *et al.*, *Ab initio three-loop calculation of the W -exchange contribution to nonleptonic decays of double charm baryons*, Phys. Rev. **D99** (2019) 056013, [arXiv:1812.09212](#).
- [19] T. Gutsche, M. A. Ivanov, J. G. Körner, and V. E. Lyubovitskij, *Decay chain information on the newly discovered double charm baryon state Ξ_{cc}^{++}* , Phys. Rev. **D96** (2017) 054013, [arXiv:1708.00703](#).
- [20] T. Gutsche *et al.*, *Analysis of the semileptonic and nonleptonic two-body decays of the double heavy charm baryon states Ξ_{cc}^{++} , Ξ_{cc}^+ and Ω_{cc}^+* , Phys. Rev. **D100** (2019) 114037, [arXiv:1911.10785](#).
- [21] M. A. Ivanov, J. G. Körner, and V. E. Lyubovitskij, *Nonleptonic decays of doubly charmed baryons*, Phys. Part. Nucl. **51** (2020) 678.
- [22] H.-Y. Cheng, G. Meng, F. Xu, and J. Zou, *Two-body weak decays of doubly charmed baryons*, Phys. Rev. **D101** (2020) 034034, [arXiv:2001.04553](#).
- [23] LHCb collaboration, A. A. Alves Jr. *et al.*, *The LHCb detector at the LHC*, JINST **3** (2008) S08005.
- [24] LHCb collaboration, R. Aaij *et al.*, *LHCb detector performance*, Int. J. Mod. Phys. **A30** (2015) 1530022, [arXiv:1412.6352](#).
- [25] R. Aaij *et al.*, *The LHCb trigger and its performance in 2011*, JINST **8** (2013) P04022, [arXiv:1211.3055](#).
- [26] T. Sjöstrand, S. Mrenna, and P. Skands, *A brief introduction to PYTHIA 8.1*, Comput. Phys. Commun. **178** (2008) 852, [arXiv:0710.3820](#); T. Sjöstrand, S. Mrenna, and P. Skands, *PYTHIA 6.4 physics and manual*, JHEP **05** (2006) 026, [arXiv:hep-ph/0603175](#).

- [27] I. Belyaev *et al.*, *Handling of the generation of primary events in Gauss, the LHCb simulation framework*, J. Phys. Conf. Ser. **331** (2011) 032047.
- [28] C.-H. Chang, J.-X. Wang, and X.-G. Wu, *GENXICC2.0: an upgraded version of the generator for hadronic production of double heavy baryons Ξ_{cc} , Ξ_{bc} and Ξ_{bb}* , Comput. Phys. Commun. **181** (2010) 1144, [arXiv:0910.4462](#).
- [29] D. J. Lange, *The EvtGen particle decay simulation package*, Nucl. Instrum. Meth. **A462** (2001) 152.
- [30] N. Davidson, T. Przedzinski, and Z. Was, *PHOTOS interface in C++: Technical and physics documentation*, Comp. Phys. Comm. **199** (2016) 86, [arXiv:1011.0937](#).
- [31] Geant4 collaboration, J. Allison *et al.*, *Geant4 developments and applications*, IEEE Trans. Nucl. Sci. **53** (2006) 270.
- [32] H. Schreiner *et al.*, *A Python upgrade to the GooFit package for parallel fitting*, EPJ Web Conf. **214** (2019) 05006.
- [33] G. A. Cowan, D. C. Craik, and M. D. Needham, *RapidSim: an application for the fast simulation of heavy-quark hadron decays*, Comput. Phys. Commun. **214** (2017) 239, [arXiv:1612.07489](#).
- [34] A. Hoecker *et al.*, *TMVA 4 — Toolkit for Multivariate Data Analysis with ROOT. Users Guide.*, [arXiv:physics/0703039](#).
- [35] Particle Data Group, P. A. Zyla *et al.*, *Review of particle physics*, Prog. Theor. Exp. Phys. **2020** (2020) 083C01.
- [36] T. Skwarnicki, *A study of the radiative cascade transitions between the Upsilon-prime and Upsilon resonances*, PhD thesis, Institute of Nuclear Physics, Krakow, 1986, DESY-F31-86-02.
- [37] M. Pivk and F. R. Le Diberder, *SPlot: A Statistical tool to unfold data distributions*, Nucl. Instrum. Meth. **A555** (2005) 356, [arXiv:physics/0402083](#).
- [38] R. Aaij *et al.*, *Selection and processing of calibration samples to measure the particle identification performance of the LHCb experiment in Run 2*, Eur. Phys. J. Tech. Instr. **6** (2019) 1, [arXiv:1803.00824](#).
- [39] L. Lyons, D. Gibaut, and P. Clifford, *How to combine correlated estimates of a single physical quantity*, Nucl. Instrum. Meth. **A270** (1988) 110.
- [40] A. Valassi, *Combining correlated measurements of several different physical quantities*, Nucl. Instrum. Meth. **A500** (2003) 391.

LHCb collaboration

319 R. Aaij³², A.S.W. Abdelmotteleb⁵⁶, C. Abellán Beteta⁵⁰, F. Abudinén⁵⁶, T. Ackernley⁶⁰,
 320 B. Adeva⁴⁶, M. Adinolfi⁵⁴, H. Afsharnia⁹, C. Agapopoulou¹³, C.A. Aidala⁸⁷, S. Aiola²⁵,
 321 Z. Ajaltouni⁹, S. Akar⁶⁵, J. Albrecht¹⁵, F. Alessio⁴⁸, M. Alexander⁵⁹, A. Alfonso Alberio⁴⁵,
 322 Z. Aliouche⁶², G. Alkhazov³⁸, P. Alvarez Cartelle⁵⁵, S. Amato², J.L. Amey⁵⁴, Y. Amhis¹¹,
 323 L. An⁴⁸, L. Anderlini²², M. Andersson⁵⁰, A. Andreianov³⁸, M. Andreotti²¹, F. Archilli¹⁷,
 324 A. Artamonov⁴⁴, M. Artuso⁶⁸, K. Arzymatov⁴², E. Aslanides¹⁰, M. Atzeni⁵⁰, B. Audurier¹²,
 325 S. Bachmann¹⁷, M. Bachmayer⁴⁹, J.J. Back⁵⁶, P. Baladron Rodriguez⁴⁶, V. Balagura¹²,
 326 W. Baldini²¹, J. Baptista de Souza Leite¹, M. Barbetti^{22,h}, R.J. Barlow⁶², S. Barsuk¹¹,
 327 W. Barter⁶¹, M. Bartolini⁵⁵, F. Baryshnikov⁸³, J.M. Basels¹⁴, S. Bashir³⁴, G. Bassi²⁹,
 328 B. Batsukh⁴, A. Battig¹⁵, A. Bay⁴⁹, A. Beck⁵⁶, M. Becker¹⁵, F. Bedeschi²⁹, I. Bediaga¹,
 329 A. Beiter⁶⁸, V. Belavin⁴², S. Belin⁴⁶, V. Belle⁵⁰, K. Belous⁴⁴, I. Belov⁴⁰, I. Belyaev⁴¹,
 330 G. Bencivenni²³, E. Ben-Haim¹³, A. Berezhniov⁴⁰, R. Bernet⁵⁰, D. Berninghoff¹⁷,
 331 H.C. Bernstein⁶⁸, C. Bertella⁶², A. Bertolin²⁸, C. Betancourt⁵⁰, F. Betti⁴⁸, Ia. Bezshyiko⁵⁰,
 332 S. Bhasin⁵⁴, J. Bhom³⁵, L. Bian⁷³, M.S. Bieker¹⁵, N.V. Biesuz²¹, S. Bifani⁵³, P. Billoir¹³,
 333 A. Biolchini³², M. Birch⁶¹, F.C.R. Bishop⁵⁵, A. Bitadze⁶², A. Bizzeti^{22,l}, M. Bjørn⁶³,
 334 M.P. Blago⁵⁵, T. Blake⁵⁶, F. Blanc⁴⁹, S. Blusk⁶⁸, D. Bobulska⁵⁹, J.A. Boelhaue¹⁵,
 335 O. Boente Garcia⁴⁶, T. Boettcher⁶⁵, A. Boldyrev⁸², A. Bondar⁴³, N. Bondar^{38,48}, S. Borghi⁶²,
 336 M. Borisov⁴², M. Borsato¹⁷, J.T. Borsuk³⁵, S.A. Bouchiba⁴⁹, T.J.V. Bowcock^{60,48}, A. Boyer⁴⁸,
 337 C. Bozzi²¹, M.J. Bradley⁶¹, S. Braun⁶⁶, A. Brea Rodriguez⁴⁶, J. Brodzicka³⁵,
 338 A. Brossa Gonzalo⁵⁶, D. Brundu²⁷, A. Buonauro⁵⁰, L. Buonincontri²⁸, A.T. Burke⁶², C. Burr⁴⁸,
 339 A. Bursche⁷², A. Butkevich³⁹, J.S. Butter³², J. Buytaert⁴⁸, W. Byczynski⁴⁸, S. Cadeddu²⁷,
 340 H. Cai⁷³, R. Calabrese^{21,g}, L. Calefice^{15,13}, S. Cali²³, R. Calladine⁵³, M. Calvi^{26,k},
 341 M. Calvo Gomez⁸⁵, P. Camargo Magalhaes⁵⁴, P. Campana²³, A.F. Campoverde Quezada⁶,
 342 S. Capelli^{26,k}, L. Capriotti^{20,e}, A. Carbone^{20,e}, G. Carboni^{31,q}, R. Cardinale^{24,i}, A. Cardini²⁷,
 343 I. Carli⁴, P. Carniti^{26,k}, L. Carus¹⁴, K. Carvalho Akiba³², A. Casais Vidal⁴⁶, R. Caspary¹⁷,
 344 G. Casse⁶⁰, M. Cattaneo⁴⁸, G. Cavallero⁴⁸, S. Celani⁴⁹, J. Cerasoli¹⁰, D. Cervenkov⁶³,
 345 A.J. Chadwick⁶⁰, M.G. Chapman⁵⁴, M. Charles¹³, Ph. Charpentier⁴⁸, C.A. Chavez Barajas⁶⁰,
 346 M. Chefdeville⁸, C. Chen³, S. Chen⁴, A. Chernov³⁵, V. Chobanova⁴⁶, S. Cholak⁴⁹,
 347 M. Chruszcz³⁵, A. Chubykin³⁸, V. Chulikov³⁸, P. Ciambrone²³, M.F. Cicala⁵⁶, X. Cid Vidal⁴⁶,
 348 G. Ciezarek⁴⁸, P.E.L. Clarke⁵⁸, M. Clemencic⁴⁸, H.V. Cliff⁵⁵, J. Closier⁴⁸, J.L. Cobbledick⁶²,
 349 V. Coco⁴⁸, J.A.B. Coelho¹¹, J. Cogan¹⁰, E. Cogneras⁹, L. Cojocariu³⁷, P. Collins⁴⁸,
 350 T. Colombo⁴⁸, L. Congedo^{19,d}, A. Contu²⁷, N. Cooke⁵³, G. Coombs⁵⁹, I. Corredoira⁴⁶,
 351 G. Corti⁴⁸, C.M. Costa Sobral⁵⁶, B. Couturier⁴⁸, D.C. Craik⁶⁴, J. Crkovská⁶⁷, M. Cruz Torres¹,
 352 R. Currie⁵⁸, C.L. Da Silva⁶⁷, S. Dadabaev⁸³, L. Dai⁷¹, E. Dall'Occo¹⁵, J. Dalseno⁴⁶,
 353 C. D'Ambrosio⁴⁸, A. Danilina⁴¹, P. d'Argent⁴⁸, A. Dashkina⁸³, J.E. Davies⁶², A. Davis⁶²,
 354 O. De Aguiar Francisco⁶², K. De Bruyn⁷⁹, S. De Capua⁶², M. De Cian⁴⁹,
 355 U. De Freitas Carneiro Da Graca¹, E. De Lucia²³, J.M. De Miranda¹, L. De Paula²,
 356 M. De Serio^{19,d}, D. De Simone⁵⁰, P. De Simone²³, F. De Vellis¹⁵, J.A. de Vries⁸⁰, C.T. Dean⁶⁷,
 357 F. Debernardis^{19,d}, D. Decamp⁸, V. Dedu¹⁰, L. Del Buono¹³, B. Delaney⁵⁵, H.-P. Dembinski¹⁵,
 358 V. Denysenko⁵⁰, D. Derkach⁸², O. Deschamps⁹, F. Dettori^{27,f}, B. Dey⁷⁷, A. Di Cicco²³,
 359 P. Di Nezza²³, S. Didenko⁸³, L. Dieste Maronas⁴⁶, S. Ding⁶⁸, V. Dobishuk⁵², C. Dong³,
 360 A.M. Donohoe¹⁸, F. Dordei²⁷, A.C. dos Reis¹, L. Douglas⁵⁹, A. Dovbnya⁵¹, A.G. Downes⁸,
 361 M.W. Dudek³⁵, L. Dufour⁴⁸, V. Duk⁷⁸, P. Durante⁴⁸, J.M. Durham⁶⁷, D. Dutta⁶²,
 362 A. Dziurda³⁵, A. Dzyuba³⁸, S. Easo⁵⁷, U. Egede⁶⁹, V. Egorychev⁴¹, S. Eidelman^{43,u,†},
 363 S. Eisenhardt⁵⁸, S. Ek-In⁴⁹, L. Eklund⁸⁶, S. Ely⁶⁸, A. Ene³⁷, E. Eppe⁶⁷, S. Escher¹⁴,
 364 J. Eschle⁵⁰, S. Esen⁵⁰, T. Evans⁶², L.N. Falcao¹, Y. Fan⁶, B. Fang⁷³, S. Farry⁶⁰, D. Fazzini^{26,k},
 365 M. Féo⁴⁸, A. Fernandez Prieto⁴⁶, A.D. Fernez⁶⁶, F. Ferrari²⁰, L. Ferreira Lopes⁴⁹,
 366 F. Ferreira Rodrigues², S. Ferreres Sole³², M. Ferrillo⁵⁰, M. Ferro-Luzzi⁴⁸, S. Filippov³⁹,

367 R.A. Fini¹⁹, M. Fiorini^{21,g}, M. Firlej³⁴, K.M. Fischer⁶³, D.S. Fitzgerald⁸⁷, C. Fitzpatrick⁶²,
 368 T. Fiutowski³⁴, A. Fkias⁴⁸, F. Fleuret¹², M. Fontana¹³, F. Fontanelli^{24,i}, R. Forty⁴⁸,
 369 D. Foulds-Holt⁵⁵, V. Franco Lima⁶⁰, M. Franco Sevilla⁶⁶, M. Frank⁴⁸, E. Franzoso²¹, G. Frau¹⁷,
 370 C. Frei⁴⁸, D.A. Friday⁵⁹, J. Fu⁶, Q. Fuehring¹⁵, E. Gabriel³², G. Galati^{19,d}, A. Gallas Torreira⁴⁶,
 371 D. Galli^{20,e}, S. Gambetta^{58,48}, Y. Gan³, M. Gandelman², P. Gandini²⁵, Y. Gao⁵, M. Garau²⁷,
 372 L.M. Garcia Martin⁵⁶, P. Garcia Moreno⁴⁵, J. García Pardiñas^{26,k}, B. Garcia Plana⁴⁶,
 373 F.A. Garcia Rosales¹², L. Garrido⁴⁵, C. Gaspar⁴⁸, R.E. Geertsema³², D. Gerick¹⁷,
 374 L.L. Gerken¹⁵, E. Gersabeck⁶², M. Gersabeck⁶², T. Gershon⁵⁶, L. Giambastiani²⁸, V. Gibson⁵⁵,
 375 H.K. Giemza³⁶, A.L. Gilman⁶³, M. Giovannetti^{23,q}, A. Gioventù⁴⁶, P. Gironella Gironell⁴⁵,
 376 C. Giugliano²¹, K. Gizdov⁵⁸, E.L. Gkougkousis⁴⁸, V.V. Gligorov^{13,48}, C. Göbel⁷⁰,
 377 E. Golobardes⁸⁵, D. Golubkov⁴¹, A. Golutvin^{61,83}, A. Gomes^{1,a}, S. Gomez Fernandez⁴⁵,
 378 F. Goncalves Abrantes⁶³, M. Goncerz³⁵, G. Gong³, P. Gorbounov⁴¹, I.V. Gorelov⁴⁰, C. Gotti²⁶,
 379 J.P. Grabowski¹⁷, T. Grammatico¹³, L.A. Granado Cardoso⁴⁸, E. Graugés⁴⁵, E. Graverini⁴⁹,
 380 G. Graziani²², A. Grecu³⁷, L.M. Greeven³², N.A. Grieser⁴, L. Grillo⁶², S. Gromov⁸³,
 381 B.R. Gruberg Cazon⁶³, C. Gu³, M. Guarise²¹, M. Guittiere¹¹, P. A. Günther¹⁷, E. Gushchin³⁹,
 382 A. Guth¹⁴, Y. Guz⁴⁴, T. Gys⁴⁸, T. Hadavizadeh⁶⁹, G. Haefeli⁴⁹, C. Haen⁴⁸, J. Haimberger⁴⁸,
 383 S.C. Haines⁵⁵, T. Halewood-leagas⁶⁰, P.M. Hamilton⁶⁶, J.P. Hammerich⁶⁰, Q. Han⁷, X. Han¹⁷,
 384 E.B. Hansen⁶², S. Hansmann-Menzemer^{17,48}, N. Harnew⁶³, T. Harrison⁶⁰, C. Hasse⁴⁸,
 385 M. Hatch⁴⁸, J. He^{6,b}, K. Heijhoff³², K. Heinicke¹⁵, R.D.L. Henderson^{69,56}, A.M. Hennequin⁶⁴,
 386 K. Hennessy⁶⁰, L. Henry⁴⁸, J. Heuel¹⁴, A. Hicheur², D. Hill⁴⁹, M. Hilton⁶², S.E. Hollitt¹⁵,
 387 R. Hou⁷, Y. Hou⁸, J. Hu¹⁷, J. Hu⁷², W. Hu⁷, X. Hu³, W. Huang⁶, X. Huang⁷³,
 388 W. Hulsbergen³², R.J. Hunter⁵⁶, M. Hushchyn⁸², D. Hutchcroft⁶⁰, D. Hynds³², P. Ibis¹⁵,
 389 M. Idzik³⁴, D. Ilin³⁸, P. Ilten⁶⁵, A. Inglessi³⁸, A. Iniukhin⁸², A. Ishteev⁸³, K. Ivshin³⁸,
 390 R. Jacobsson⁴⁸, H. Jage¹⁴, S. Jakobsen⁴⁸, E. Jans³², B.K. Jashal⁴⁷, A. Jawahery⁶⁶, V. Jevtic¹⁵,
 391 X. Jiang⁴, M. John⁶³, D. Johnson⁶⁴, C.R. Jones⁵⁵, T.P. Jones⁵⁶, B. Jost⁴⁸, N. Jurik⁴⁸,
 392 S.H. Kalavan Kadavath³⁴, S. Kandybei⁵¹, Y. Kang³, M. Karacson⁴⁸, D. Karpenkov⁸³,
 393 M. Karpov⁸², J.W. Kautz⁶⁵, F. Keizer⁴⁸, D.M. Keller⁶⁸, M. Kenzie⁵⁶, T. Ketel³³, B. Khanji¹⁵,
 394 A. Kharisova⁸⁴, S. Kholodenko^{44,83}, T. Kirn¹⁴, V.S. Kirsebom⁴⁹, O. Kitouni⁶⁴, S. Klaver³³,
 395 N. Kleijne²⁹, K. Klimaszewski³⁶, M.R. Kmiec³⁶, S. Kolliiev⁵², A. Kondybayeva⁸³,
 396 A. Konoplyannikov⁴¹, P. Kopciwicz³⁴, R. Kopečna¹⁷, P. Koppenburg³², M. Korolev⁴⁰,
 397 I. Kostiuk^{32,52}, O. Kot⁵², S. Kotriakhova^{21,38}, A. Kozachuk⁴⁰, P. Kravchenko³⁸, L. Kravchuk³⁹,
 398 R.D. Krawczyk⁴⁸, M. Kreps⁵⁶, S. Kretzschmar¹⁴, P. Krokovny^{43,u}, W. Krupa³⁴, W. Krzemien³⁶,
 399 J. Kubat¹⁷, M. Kucharczyk³⁵, V. Kudryavtsev^{43,u}, H.S. Kuindersma^{32,33}, G.J. Kunde⁶⁷,
 400 T. Kvaratskheliya⁴¹, D. Lacarrere⁴⁸, G. Lafferty⁶², A. Lai²⁷, A. Lampis²⁷, D. Lancierini⁵⁰,
 401 J.J. Lane⁶², R. Lane⁵⁴, G. Lanfranchi²³, C. Langenbruch¹⁴, J. Langer¹⁵, O. Lantwin⁸³,
 402 T. Latham⁵⁶, F. Lazzari²⁹, R. Le Gac¹⁰, S.H. Lee⁸⁷, R. Lefèvre⁹, A. Leflat⁴⁰, S. Legotin⁸³,
 403 O. Leroy¹⁰, T. Lesiak³⁵, B. Leverington¹⁷, H. Li⁷², P. Li¹⁷, S. Li⁷, Y. Li⁴, Z. Li⁶⁸, X. Liang⁶⁸,
 404 T. Lin⁶¹, R. Lindner⁴⁸, V. Lisovsky¹⁵, R. Litvinov²⁷, G. Liu⁷², H. Liu⁶, Q. Liu⁶, S. Liu⁴,
 405 A. Lobo Salvia⁴⁵, A. Loi²⁷, R. Lollini⁷⁸, J. Lomba Castro⁴⁶, I. Longstaff⁵⁹, J.H. Lopes²,
 406 S. López Soliño⁴⁶, G.H. Lovell⁵⁵, Y. Lu⁴, C. Lucarelli^{22,h}, D. Lucchesi^{28,m}, S. Luchuk³⁹,
 407 M. Lucio Martinez³², V. Lukashenko^{32,52}, Y. Luo³, A. Lupato⁶², E. Luppi^{21,g}, O. Lupton⁵⁶,
 408 A. Lusiani^{29,n}, X. Lyu⁶, L. Ma⁴, R. Ma⁶, S. Maccolini²⁰, F. Machefert¹¹, F. Maciuc³⁷,
 409 V. Macko⁴⁹, P. Mackowiak¹⁵, S. Maddrell-Mander⁵⁴, O. Madejczyk³⁴, L.R. Madhan Mohan⁵⁴,
 410 O. Maev³⁸, A. Maevskiy⁸², D. Maisuzenko³⁸, M.W. Majewski³⁴, J.J. Malczewski³⁵, S. Malde⁶³,
 411 B. Malecki³⁵, A. Malinin⁸¹, T. Maltsev^{43,u}, H. Malygina¹⁷, G. Manca^{27,f}, G. Mancinelli¹⁰,
 412 D. Manuzzi²⁰, C.A. Manzari⁵⁰, D. Marangotto^{25,j}, J. Maratas^{9,s}, J.F. Marchand⁸, U. Marconi²⁰,
 413 S. Mariani^{22,h}, C. Marin Benito⁴⁸, M. Marinangeli⁴⁹, J. Marks¹⁷, A.M. Marshall⁵⁴,
 414 P.J. Marshall⁶⁰, G. Martelli⁷⁸, G. Martellotti³⁰, L. Martinazzoli^{48,k}, M. Martinelli^{26,k},
 415 D. Martinez Santos⁴⁶, F. Martinez Vidal⁴⁷, A. Massafferri¹, M. Materok¹⁴, R. Matev⁴⁸,
 416 A. Mathad⁵⁰, V. Matiunin⁴¹, C. Matteuzzi²⁶, K.R. Mattioli⁸⁷, A. Mauri³², E. Maurice¹²,

417 J. Mauricio⁴⁵, M. Mazurek⁴⁸, M. McCann⁶¹, L. McConnell¹⁸, T.H. Mcgrath⁶², N.T. Mchugh⁵⁹,
 418 A. McNab⁶², R. McNulty¹⁸, J.V. Mead⁶⁰, B. Meadows⁶⁵, G. Meier¹⁵, D. Melnychuk³⁶,
 419 S. Meloni^{26,k}, M. Merk^{32,80}, A. Merli^{25,j}, L. Meyer Garcia², M. Mikhasenko^{75,c}, D.A. Milanes⁷⁴,
 420 E. Millard⁵⁶, M. Milovanovic⁴⁸, M.-N. Minard⁸, A. Minotti^{26,k}, S.E. Mitchell⁵⁸, B. Mitreska⁶²,
 421 D.S. Mitzel¹⁵, A. Mödden¹⁵, R.A. Mohammed⁶³, R.D. Moise⁶¹, S. Mokhnenko⁸²,
 422 T. Mombächer⁴⁶, I.A. Monroy⁷⁴, S. Monteil⁹, M. Morandin²⁸, G. Morello²³, M.J. Morello^{29,n},
 423 J. Moron³⁴, A.B. Morris⁷⁵, A.G. Morris⁵⁶, R. Mountain⁶⁸, H. Mu³, F. Muheim⁵⁸, M. Mulder⁷⁹,
 424 K. Müller⁵⁰, C.H. Murphy⁶³, D. Murray⁶², R. Murta⁶¹, P. Muzzetto²⁷, P. Naik⁵⁴, T. Nakada⁴⁹,
 425 R. Nandakumar⁵⁷, T. Nanut⁴⁸, I. Nasteva², M. Needham⁵⁸, N. Neri^{25,j}, S. Neubert⁷⁵,
 426 N. Neufeld⁴⁸, R. Newcombe⁶¹, E.M. Niel⁴⁹, S. Nieswand¹⁴, N. Nikitin⁴⁰, N.S. Nolte⁶⁴,
 427 C. Normand⁸, C. Nunez⁸⁷, A. Oblakowska-Mucha³⁴, V. Obraztsov⁴⁴, T. Oeser¹⁴,
 428 D.P. O’Hanlon⁵⁴, S. Okamura²¹, R. Oldeman^{27,f}, F. Oliva⁵⁸, M.E. Olivares⁶⁸,
 429 C.J.G. Onderwater⁷⁹, R.H. O’Neil⁵⁸, J.M. Otalora Goicochea², T. Ovsiannikova⁴¹, P. Owen⁵⁰,
 430 A. Oyanguren⁴⁷, O. Ozcelik⁵⁸, K.O. Padeken⁷⁵, B. Pagare⁵⁶, P.R. Pais⁴⁸, T. Pajero⁶³,
 431 A. Palano¹⁹, M. Palutan²³, Y. Pan⁶², G. Panshin⁸⁴, A. Papanestis⁵⁷, M. Pappagallo^{19,d},
 432 L.L. Pappalardo²¹, C. Pappenheimer⁶⁵, W. Parker⁶⁶, C. Parkes⁶², B. Passalacqua²¹,
 433 G. Passaleva²², A. Pastore¹⁹, M. Patel⁶¹, C. Patrignani^{20,e}, C.J. Pawley⁸⁰, A. Pearce^{48,57},
 434 A. Pellegrino³², M. Pepe Altarelli⁴⁸, S. Perazzini²⁰, D. Pereima⁴¹, A. Pereiro Castro⁴⁶,
 435 P. Perret⁹, M. Petric^{59,48}, K. Petridis⁵⁴, A. Petrolini^{24,i}, A. Petrov⁸¹, S. Petrucci⁵⁸,
 436 M. Petruzzo²⁵, T.T.H. Pham⁶⁸, A. Philippov⁴², R. Piandani⁶, L. Pica^{29,n}, M. Piccini⁷⁸,
 437 B. Pietrzyk⁸, G. Pietrzyk¹¹, M. Pili⁶³, D. Pinci³⁰, F. Pisani⁴⁸, M. Pizzichemi^{26,48,k}, Resmi
 438 P.K¹⁰, V. Placinta³⁷, J. Plews⁵³, M. Plo Casasus⁴⁶, F. Polci^{13,48}, M. Poli Lener²³,
 439 M. Poliakova⁶⁸, A. Poluektov¹⁰, N. Polukhina^{83,t}, I. Polyakov⁶⁸, E. Polycarpo², S. Ponce⁴⁸,
 440 D. Popov^{6,48}, S. Popov⁴², S. Poslavskii⁴⁴, K. Prasanth³⁵, L. Promberger⁴⁸, C. Prouve⁴⁶,
 441 V. Pugatch⁵², V. Puill¹¹, G. Punzi^{29,o}, H. Qi³, W. Qian⁶, N. Qin³, R. Quagliani⁴⁹, N.V. Raab¹⁸,
 442 R.I. Rabadan Trejo⁶, B. Rachwal³⁴, J.H. Rademacker⁵⁴, R. Rajagopalan⁶⁸, M. Rama²⁹,
 443 M. Ramos Pernas⁵⁶, M.S. Rangel², F. Ratnikov^{42,82}, G. Raven^{33,48}, M. Reboud⁸, F. Redi⁴⁸,
 444 F. Reiss⁶², C. Remon Alepuz⁴⁷, Z. Ren³, V. Renaudin⁶³, R. Ribatti²⁹, A.M. Ricci²⁷,
 445 S. Ricciardi⁵⁷, K. Rinnert⁶⁰, P. Robbe¹¹, G. Robertson⁵⁸, A.B. Rodrigues⁴⁹, E. Rodrigues⁶⁰,
 446 J.A. Rodriguez Lopez⁷⁴, E.R.R. Rodriguez Rodriguez⁴⁶, A. Rollings⁶³, P. Roloff⁴⁸,
 447 V. Romanovskiy⁴⁴, M. Romero Lamas⁴⁶, A. Romero Vidal⁴⁶, J.D. Roth⁸⁷, M. Rotondo²³,
 448 M.S. Rudolph⁶⁸, T. Ruf⁴⁸, R.A. Ruiz Fernandez⁴⁶, J. Ruiz Vidal⁴⁷, A. Ryzhikov⁸², J. Ryzka³⁴,
 449 J.J. Saborido Silva⁴⁶, N. Sagidova³⁸, N. Sahoo⁵³, B. Saitta^{27,f}, M. Salomoni⁴⁸,
 450 C. Sanchez Gras³², I. Sanderswood⁴⁷, R. Santacesaria³⁰, C. Santamarina Rios⁴⁶,
 451 M. Santimaria²³, E. Santovetti^{31,q}, D. Saranin⁸³, G. Sarpis¹⁴, M. Sarpis⁷⁵, A. Sarti³⁰,
 452 C. Satriano^{30,p}, A. Satta³¹, M. Saur¹⁵, D. Savrina^{41,40}, H. Sazak⁹, L.G. Scantlebury Smead⁶³,
 453 A. Scarabotto¹³, S. Schael¹⁴, S. Scherl⁶⁰, M. Schiller⁵⁹, H. Schindler⁴⁸, M. Schmelling¹⁶,
 454 B. Schmidt⁴⁸, S. Schmitt¹⁴, O. Schneider⁴⁹, A. Schopper⁴⁸, M. Schubiger³², S. Schulte⁴⁹,
 455 M.H. Schune¹¹, R. Schwemmer⁴⁸, B. Sciascia^{23,48}, S. Sellam⁴⁶, A. Semennikov⁴¹,
 456 M. Senghi Soares³³, A. Sergi^{24,i}, N. Serra⁵⁰, L. Sestini²⁸, A. Seuthe¹⁵, Y. Shang⁵,
 457 D.M. Shangase⁸⁷, M. Shapkin⁴⁴, I. Shchemerov⁸³, L. Shchutska⁴⁹, T. Shears⁶⁰,
 458 L. Shekhtman^{43,u}, Z. Shen⁵, S. Sheng⁴, V. Shevchenko⁸¹, E.B. Shields^{26,k}, Y. Shimizu¹¹,
 459 E. Shmanin⁸³, J.D. Shupperd⁶⁸, B.G. Siddi²¹, R. Silva Coutinho⁵⁰, G. Simi²⁸, S. Simone^{19,d},
 460 M. Singla⁶⁹, N. Skidmore⁶², R. Skuza¹⁷, T. Skwarnicki⁶⁸, M.W. Slater⁵³, I. Slazyk^{21,g},
 461 J.C. Smallwood⁶³, J.G. Smeaton⁵⁵, E. Smith⁵⁰, M. Smith⁶¹, A. Snoch³², L. Soares Lavra⁹,
 462 M.D. Sokoloff⁶⁵, F.J.P. Soler⁵⁹, A. Solovev³⁸, I. Solovyevev³⁸, F.L. Souza De Almeida²,
 463 B. Souza De Paula², B. Spaan¹⁵, E. Spadaro Norella^{25,j}, P. Spradlin⁵⁹, F. Stagni⁴⁸, M. Stahl⁶⁵,
 464 S. Stahl⁴⁸, S. Stanislaus⁶³, O. Steinkamp^{50,83}, O. Stenyakin⁴⁴, H. Stevens¹⁵, S. Stone^{68,48,†},
 465 D. Strelakina⁸³, F. Suljik⁶³, J. Sun²⁷, L. Sun⁷³, Y. Sun⁶⁶, P. Sviha⁶², P.N. Swallow⁵³,
 466 K. Swientek³⁴, A. Szabelski³⁶, T. Szumlak³⁴, M. Szymanski⁴⁸, S. Taneja⁶², A.R. Tanner⁵⁴,

467 M.D. Tat⁶³, A. Terentev⁸³, F. Teubert⁴⁸, E. Thomas⁴⁸, D.J.D. Thompson⁵³, K.A. Thomson⁶⁰,
 468 H. Tilquin⁶¹, V. Tisserand⁹, S. T'Jampens⁸, M. Tobin⁴, L. Tomassetti^{21,g}, X. Tong⁵,
 469 D. Torres Machado¹, D.Y. Tou³, E. Trifonova⁸³, S.M. Trilov⁵⁴, C. Trippi⁴⁹, G. Tuci⁶, A. Tully⁴⁹,
 470 N. Tuning^{32,48}, A. Ukleja³⁶, D.J. Unverzagt¹⁷, E. Ursov⁸³, A. Usachov³², A. Ustyuzhanin^{42,82},
 471 U. Uwer¹⁷, A. Vagner⁸⁴, V. Vagnoni²⁰, A. Valassi⁴⁸, G. Valenti²⁰, N. Valls Canudas⁸⁵,
 472 M. van Beuzekom³², M. Van Dijk⁴⁹, H. Van Hecke⁶⁷, E. van Herwijnen⁸³, M. van Veghel⁷⁹,
 473 R. Vazquez Gomez⁴⁵, P. Vazquez Regueiro⁴⁶, C. Vázquez Sierra⁴⁸, S. Vecchi²¹, J.J. Velthuis⁵⁴,
 474 M. Veltri^{22,r}, A. Venkateswaran⁶⁸, M. Veronesi³², M. Vesterinen⁵⁶, D. Vieira⁶⁵,
 475 M. Vieites Diaz⁴⁹, H. Viemann⁷⁶, X. Vilasis-Cardona⁸⁵, E. Vilella Figueras⁶⁰, A. Villa²⁰,
 476 P. Vincent¹³, F.C. Volle¹¹, D. Vom Bruch¹⁰, A. Vorobyev³⁸, V. Vorobyev^{43,u}, N. Voropaev³⁸,
 477 K. Vos⁸⁰, R. Waldi¹⁷, J. Walsh²⁹, C. Wang¹⁷, J. Wang⁵, J. Wang⁴, J. Wang³, J. Wang⁷³,
 478 M. Wang³, R. Wang⁵⁴, Y. Wang⁷, Z. Wang⁵⁰, Z. Wang³, Z. Wang⁶, J.A. Ward^{56,69},
 479 N.K. Watson⁵³, D. Websdale⁶¹, C. Weisser⁶⁴, B.D.C. Westhenry⁵⁴, D.J. White⁶²,
 480 M. Whitehead⁵⁴, A.R. Wiederhold⁵⁶, D. Wiedner¹⁵, G. Wilkinson⁶³, M. Wilkinson⁶⁸,
 481 I. Williams⁵⁵, M. Williams⁶⁴, M.R.J. Williams⁵⁸, F.F. Wilson⁵⁷, W. Wislicki³⁶, M. Witek³⁵,
 482 L. Witola¹⁷, G. Wormser¹¹, S.A. Wotton⁵⁵, H. Wu⁶⁸, K. Wyllie⁴⁸, Z. Xiang⁶, D. Xiao⁷, Y. Xie⁷,
 483 A. Xu⁵, J. Xu⁶, L. Xu³, M. Xu⁵⁶, Q. Xu⁶, Z. Xu⁹, Z. Xu⁶, D. Yang³, S. Yang⁶, Y. Yang⁶,
 484 Z. Yang⁵, Z. Yang⁶⁶, Y. Yao⁶⁸, L.E. Yeomans⁶⁰, H. Yin⁷, J. Yu⁷¹, X. Yuan⁶⁸, O. Yushchenko⁴⁴,
 485 E. Zaffaroni⁴⁹, M. Zavertyaev^{16,t}, M. Zdybal³⁵, O. Zenaiev⁴⁸, M. Zeng³, D. Zhang⁷, L. Zhang³,
 486 S. Zhang⁷¹, S. Zhang⁵, Y. Zhang⁵, Y. Zhang⁶³, A. Zharkova⁸³, A. Zhelezov¹⁷, Y. Zheng⁶,
 487 T. Zhou⁵, X. Zhou⁶, Y. Zhou⁶, V. Zhovkovska¹¹, X. Zhu³, X. Zhu⁷, Z. Zhu⁶, V. Zhukov^{14,40},
 488 Q. Zou⁴, S. Zucchelli^{20,e}, D. Zuliani²⁸, G. Zunica⁶².

489 ¹ Centro Brasileiro de Pesquisas Físicas (CBPF), Rio de Janeiro, Brazil

490 ² Universidade Federal do Rio de Janeiro (UFRJ), Rio de Janeiro, Brazil

491 ³ Center for High Energy Physics, Tsinghua University, Beijing, China

492 ⁴ Institute Of High Energy Physics (IHEP), Beijing, China

493 ⁵ School of Physics State Key Laboratory of Nuclear Physics and Technology, Peking University, Beijing,
 494 China

495 ⁶ University of Chinese Academy of Sciences, Beijing, China

496 ⁷ Institute of Particle Physics, Central China Normal University, Wuhan, Hubei, China

497 ⁸ Univ. Savoie Mont Blanc, CNRS, IN2P3-LAPP, Annecy, France

498 ⁹ Université Clermont Auvergne, CNRS/IN2P3, LPC, Clermont-Ferrand, France

499 ¹⁰ Aix Marseille Univ, CNRS/IN2P3, CPPM, Marseille, France

500 ¹¹ Université Paris-Saclay, CNRS/IN2P3, IJCLab, Orsay, France

501 ¹² Laboratoire Leprince-Ringuet, CNRS/IN2P3, Ecole Polytechnique, Institut Polytechnique de Paris,
 502 Palaiseau, France

503 ¹³ LPNHE, Sorbonne Université, Paris Diderot Sorbonne Paris Cité, CNRS/IN2P3, Paris, France

504 ¹⁴ I. Physikalisches Institut, RWTH Aachen University, Aachen, Germany

505 ¹⁵ Fakultät Physik, Technische Universität Dortmund, Dortmund, Germany

506 ¹⁶ Max-Planck-Institut für Kernphysik (MPIK), Heidelberg, Germany

507 ¹⁷ Physikalisches Institut, Ruprecht-Karls-Universität Heidelberg, Heidelberg, Germany

508 ¹⁸ School of Physics, University College Dublin, Dublin, Ireland

509 ¹⁹ INFN Sezione di Bari, Bari, Italy

510 ²⁰ INFN Sezione di Bologna, Bologna, Italy

511 ²¹ INFN Sezione di Ferrara, Ferrara, Italy

512 ²² INFN Sezione di Firenze, Firenze, Italy

513 ²³ INFN Laboratori Nazionali di Frascati, Frascati, Italy

514 ²⁴ INFN Sezione di Genova, Genova, Italy

515 ²⁵ INFN Sezione di Milano, Milano, Italy

516 ²⁶ INFN Sezione di Milano-Bicocca, Milano, Italy

517 ²⁷ INFN Sezione di Cagliari, Monserrato, Italy

518 ²⁸ Università degli Studi di Padova, Università e INFN, Padova, Padova, Italy

519 ²⁹ INFN Sezione di Pisa, Pisa, Italy

520 ³⁰*INFN Sezione di Roma La Sapienza, Roma, Italy*
 521 ³¹*INFN Sezione di Roma Tor Vergata, Roma, Italy*
 522 ³²*Nikhef National Institute for Subatomic Physics, Amsterdam, Netherlands*
 523 ³³*Nikhef National Institute for Subatomic Physics and VU University Amsterdam, Amsterdam,*
 524 *Netherlands*
 525 ³⁴*AGH - University of Science and Technology, Faculty of Physics and Applied Computer Science,*
 526 *Kraków, Poland*
 527 ³⁵*Henryk Niewodniczanski Institute of Nuclear Physics Polish Academy of Sciences, Kraków, Poland*
 528 ³⁶*National Center for Nuclear Research (NCBJ), Warsaw, Poland*
 529 ³⁷*Horia Hulubei National Institute of Physics and Nuclear Engineering, Bucharest-Magurele, Romania*
 530 ³⁸*Petersburg Nuclear Physics Institute NRC Kurchatov Institute (PNPI NRC KI), Gatchina, Russia*
 531 ³⁹*Institute for Nuclear Research of the Russian Academy of Sciences (INR RAS), Moscow, Russia*
 532 ⁴⁰*Institute of Nuclear Physics, Moscow State University (SINP MSU), Moscow, Russia*
 533 ⁴¹*Institute of Theoretical and Experimental Physics NRC Kurchatov Institute (ITEP NRC KI), Moscow,*
 534 *Russia*
 535 ⁴²*Yandex School of Data Analysis, Moscow, Russia*
 536 ⁴³*Budker Institute of Nuclear Physics (SB RAS), Novosibirsk, Russia*
 537 ⁴⁴*Institute for High Energy Physics NRC Kurchatov Institute (IHEP NRC KI), Protvino, Russia,*
 538 *Protvino, Russia*
 539 ⁴⁵*ICCUB, Universitat de Barcelona, Barcelona, Spain*
 540 ⁴⁶*Instituto Galego de Física de Altas Enerxías (IGFAE), Universidade de Santiago de Compostela,*
 541 *Santiago de Compostela, Spain*
 542 ⁴⁷*Instituto de Física Corpuscular, Centro Mixto Universidad de Valencia - CSIC, Valencia, Spain*
 543 ⁴⁸*European Organization for Nuclear Research (CERN), Geneva, Switzerland*
 544 ⁴⁹*Institute of Physics, Ecole Polytechnique Fédérale de Lausanne (EPFL), Lausanne, Switzerland*
 545 ⁵⁰*Physik-Institut, Universität Zürich, Zürich, Switzerland*
 546 ⁵¹*NSC Kharkiv Institute of Physics and Technology (NSC KIPT), Kharkiv, Ukraine*
 547 ⁵²*Institute for Nuclear Research of the National Academy of Sciences (KINR), Kyiv, Ukraine*
 548 ⁵³*University of Birmingham, Birmingham, United Kingdom*
 549 ⁵⁴*H.H. Wills Physics Laboratory, University of Bristol, Bristol, United Kingdom*
 550 ⁵⁵*Cavendish Laboratory, University of Cambridge, Cambridge, United Kingdom*
 551 ⁵⁶*Department of Physics, University of Warwick, Coventry, United Kingdom*
 552 ⁵⁷*STFC Rutherford Appleton Laboratory, Didcot, United Kingdom*
 553 ⁵⁸*School of Physics and Astronomy, University of Edinburgh, Edinburgh, United Kingdom*
 554 ⁵⁹*School of Physics and Astronomy, University of Glasgow, Glasgow, United Kingdom*
 555 ⁶⁰*Oliver Lodge Laboratory, University of Liverpool, Liverpool, United Kingdom*
 556 ⁶¹*Imperial College London, London, United Kingdom*
 557 ⁶²*Department of Physics and Astronomy, University of Manchester, Manchester, United Kingdom*
 558 ⁶³*Department of Physics, University of Oxford, Oxford, United Kingdom*
 559 ⁶⁴*Massachusetts Institute of Technology, Cambridge, MA, United States*
 560 ⁶⁵*University of Cincinnati, Cincinnati, OH, United States*
 561 ⁶⁶*University of Maryland, College Park, MD, United States*
 562 ⁶⁷*Los Alamos National Laboratory (LANL), Los Alamos, United States*
 563 ⁶⁸*Syracuse University, Syracuse, NY, United States*
 564 ⁶⁹*School of Physics and Astronomy, Monash University, Melbourne, Australia, associated to ⁵⁶*
 565 ⁷⁰*Pontifícia Universidade Católica do Rio de Janeiro (PUC-Rio), Rio de Janeiro, Brazil, associated to ²*
 566 ⁷¹*Physics and Micro Electronic College, Hunan University, Changsha City, China, associated to ⁷*
 567 ⁷²*Guangdong Provincial Key Laboratory of Nuclear Science, Guangdong-Hong Kong Joint Laboratory of*
 568 *Quantum Matter, Institute of Quantum Matter, South China Normal University, Guangzhou, China,*
 569 *associated to ³*
 570 ⁷³*School of Physics and Technology, Wuhan University, Wuhan, China, associated to ³*
 571 ⁷⁴*Departamento de Física , Universidad Nacional de Colombia, Bogota, Colombia, associated to ¹³*
 572 ⁷⁵*Universität Bonn - Helmholtz-Institut für Strahlen und Kernphysik, Bonn, Germany, associated to ¹⁷*
 573 ⁷⁶*Institut für Physik, Universität Rostock, Rostock, Germany, associated to ¹⁷*
 574 ⁷⁷*Eotvos Lorand University, Budapest, Hungary, associated to ⁴⁸*
 575 ⁷⁸*INFN Sezione di Perugia, Perugia, Italy, associated to ²¹*

576 ⁷⁹ *Van Swinderen Institute, University of Groningen, Groningen, Netherlands, associated to* ³²
 577 ⁸⁰ *Universiteit Maastricht, Maastricht, Netherlands, associated to* ³²
 578 ⁸¹ *National Research Centre Kurchatov Institute, Moscow, Russia, associated to* ⁴¹
 579 ⁸² *National Research University Higher School of Economics, Moscow, Russia, associated to* ⁴²
 580 ⁸³ *National University of Science and Technology "MISIS", Moscow, Russia, associated to* ⁴¹
 581 ⁸⁴ *National Research Tomsk Polytechnic University, Tomsk, Russia, associated to* ⁴¹
 582 ⁸⁵ *DS4DS, La Salle, Universitat Ramon Llull, Barcelona, Spain, associated to* ⁴⁵
 583 ⁸⁶ *Department of Physics and Astronomy, Uppsala University, Uppsala, Sweden, associated to* ⁵⁹
 584 ⁸⁷ *University of Michigan, Ann Arbor, United States, associated to* ⁶⁸

585 ^a *Universidade Federal do Triângulo Mineiro (UFTM), Uberaba-MG, Brazil*
 586 ^b *Hangzhou Institute for Advanced Study, UCAS, Hangzhou, China*
 587 ^c *Excellence Cluster ORIGINS, Munich, Germany*
 588 ^d *Università di Bari, Bari, Italy*
 589 ^e *Università di Bologna, Bologna, Italy*
 590 ^f *Università di Cagliari, Cagliari, Italy*
 591 ^g *Università di Ferrara, Ferrara, Italy*
 592 ^h *Università di Firenze, Firenze, Italy*
 593 ⁱ *Università di Genova, Genova, Italy*
 594 ^j *Università degli Studi di Milano, Milano, Italy*
 595 ^k *Università di Milano Bicocca, Milano, Italy*
 596 ^l *Università di Modena e Reggio Emilia, Modena, Italy*
 597 ^m *Università di Padova, Padova, Italy*
 598 ⁿ *Scuola Normale Superiore, Pisa, Italy*
 599 ^o *Università di Pisa, Pisa, Italy*
 600 ^p *Università della Basilicata, Potenza, Italy*
 601 ^q *Università di Roma Tor Vergata, Roma, Italy*
 602 ^r *Università di Urbino, Urbino, Italy*
 603 ^s *MSU - Iligan Institute of Technology (MSU-IIT), Iligan, Philippines*
 604 ^t *P.N. Lebedev Physical Institute, Russian Academy of Science (LPI RAS), Moscow, Russia*
 605 ^u *Novosibirsk State University, Novosibirsk, Russia*

606 [†] *Deceased*